AMERICAN SOCIETY FOR MICROBIOLOGY | Applied and Environmental Microbiology®

BIOTECHNOLOGY

Establishing *Butyribacterium methylotrophicum* as a Platform Organism for the Production of Biocommodities from Liquid C_1 Metabolites

Jonathan R. Humphreys,[a] Skyler D. Hebdon,[a] Holly Rohrer,[a] Lauren Magnusson,[a] Chris Urban,[a] Yi-Pei Chen,[a] Jonathan Lo[a]

[a]Biosciences Center, National Renewable Energy Laboratory, Golden, Colorado, USA

ABSTRACT Using the Wood-Ljungdahl pathway, acetogens can nonphotosynthetically fix gaseous C_1 molecules, preventing them from entering the atmosphere. Many acetogens can also grow on liquid C_1 compounds such as formate and methanol, which avoid the storage and mass transfer issues associated with gaseous C_1 compounds. Substrate redox state also plays an important role in acetogen metabolism and can modulate products formed by these organisms. *Butyribacterium methylotrophicum* is an acetogen known for its ability to synthesize longer-chained molecules such as butyrate and butanol, which have significantly higher values than acetate or ethanol, from one-carbon (C_1) compounds. We explored *B. methylotrophicum's* C_1 metabolism by varying substrates, substrate concentrations, and substrate feeding strategies to improve four-carbon product titers. Our results showed that formate utilization by *B. methylotrophicum* favored acetate production and methanol utilization favored butyrate production. Cofeeding of both substrates produced a high butyrate titer of 4 g/liter when methanol was supplied in excess to formate. Testing of formate feeding strategies, in the presence of methanol, led to further increases in the butyrate to acetate ratio. Mixotrophic growth of liquid and gaseous C_1 substrates expanded the *B. methylotrophicum* product profile, as ethanol, butanol, and lactate were produced under these conditions. We also showed that *B. methylotrophicum* is capable of producing caproate, a six-carbon product, presumably through chain elongation cycles of the reverse β-oxidation pathway. Furthermore, we demonstrated butanol production via heterologous gene expression. Our results indicate that both selection of appropriate substrates and genetic engineering play important roles in determining titers of desired products.

IMPORTANCE Acetogenic bacteria can fix single-carbon (C_1) molecules. However, improvements are needed to overcome poor product titers. *Butyribacterium methylotrophicum* can naturally ferment C_1 compounds into longer-chained molecules such as butyrate alongside traditional acetate. Here, we show that *B. methylotrophicum* can effectively grow on formate and methanol to produce high titers of butyrate. We improved ratios of butyrate to acetate through adjusted formate feeding strategies and produced higher-value six-carbon molecules. We also expanded the *B. methylotrophicum* product profile with the addition of C_1 gases, as the organism produced ethanol, butanol, and lactate. Furthermore, we developed a transformation protocol for *B. methylotrophicum* to facilitate genetic engineering of this organism for the circular bioeconomy.

KEYWORDS *Butyribacterium methylotrophicum*, chain elongation, formate, heterologous gene expression, methanol

Greenhouse gas (GHG) emissions remain a significant problem in our efforts to tackle climate change. To fully control the rate of global temperature increases, a circular carbon economy is required to keep carbon from entering the atmosphere (1, 2). Carbon, in the forms of carbon dioxide (CO_2), carbon monoxide (CO), and methane (CH_4), an be captured in a variety of ways, including but not limited to electrochemical reduction,

Editor Pablo Ivan Nikel, Novo Nordisk Foundation Center for Biosustainability

Address correspondence to Jonathan Lo, jonathan.lo@nrel.gov.

The authors declare no conflict of interest.

Received 4 December 2021
Accepted 18 January 2022
Accepted manuscript posted online 9 February 2022
Published 22 March 2022

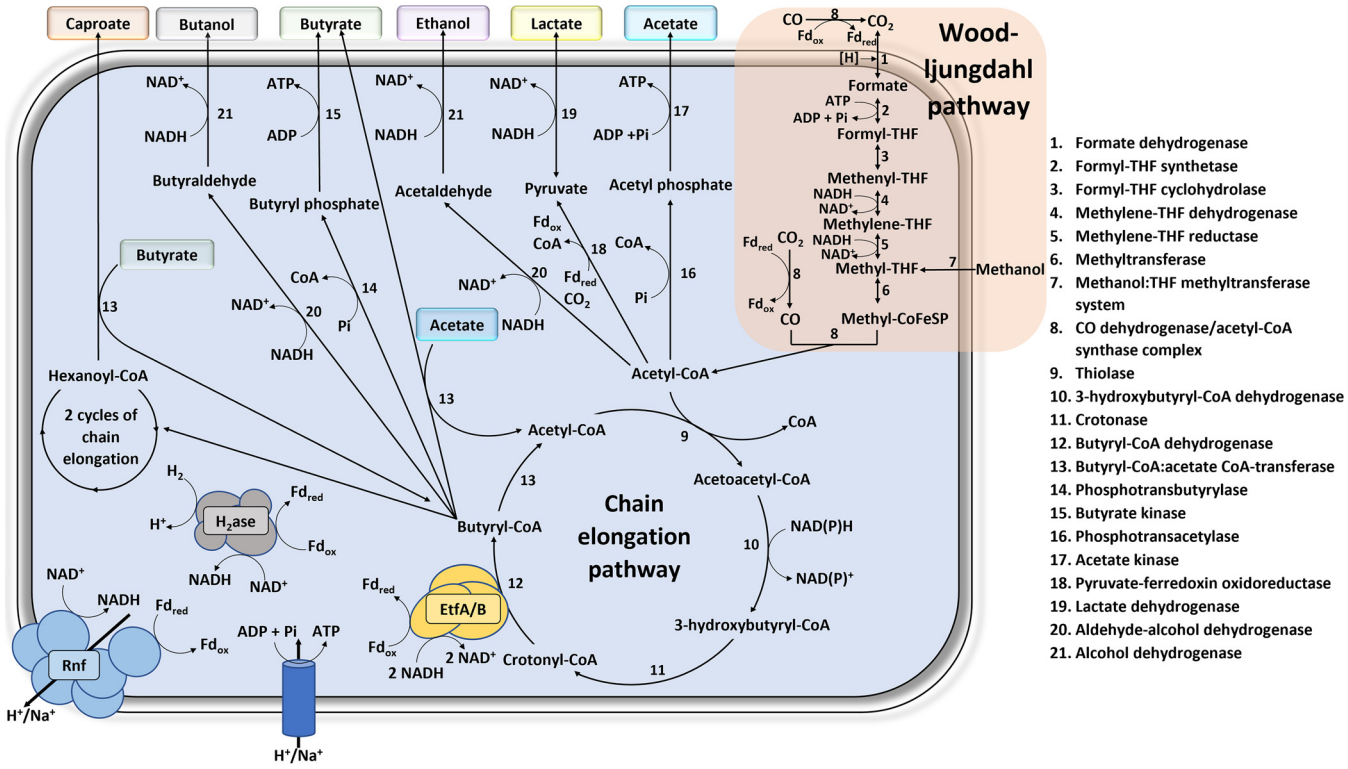

FIG 1 *B. methylotrophicum* metabolic map for all known products and C_1 substrate pathways.

thermochemical processing, and biological fixation (1, 3–6). The Wood-Ljungdahl pathway (WLP) is the most energetically efficient pathway for biological CO_2 capture and conversion (7). The WLP is an ancient metabolic pathway that allows anaerobic microorganisms, namely, acetogenic bacteria, to fix gaseous carbon to form acetyl-coenzyme A (CoA) for biomass and downstream products (8–10). The WLP consists of two branches, the carbonyl and methyl branches, that fix carbon to form the carbonyl and methyl group of acetyl-CoA, respectively (Fig. 1). The longer methyl branch consists of a variety of enzymatic steps that converts CO_2 to methyl-tetrahydrofolate (THF). Once formed, the methyl group of methyl-THF is then combined with CO (obtained from CO_2 reduction) using the CO dehydrogenase/acetyl-CoA synthase (CODH/ACS) forming acetyl-CoA (8–11).

At present, utilization of gaseous one-carbon (C_1) molecules is limited due to storage, transportation, and biological mass transfer issues (7, 12). Liquid C_1 molecules, such as formate and methanol, overcome these constraints due to their condensed state and solubility in water, making them attractive C_1 substrates for biological carbon fixation (13). Formate can be produced from CO_2 derived from waste streams, such as ethanol plants and steel mills, where the CO_2 is reduced using an electrolyzer and upgraded to a variety of chemicals including formate, ethanol, and ethylene (3, 4, 14–16). Methanol can be produced catalytically using the Fischer-Tropsch process from syn(thesis)gas (combinations of CO, CO_2, and H_2) derived from either steam-reformed natural gas (methane) or from waste gas streams. Furthermore, methanol can also be produced via CO_2 hydrogenation using hydrogen derived from the electrolysis of water (17–19). With the increasing amount of energy derived from renewable sources, renewable electricity can be used for these processes to sustain formate and methanol production (5). Once upgraded, these chemicals can be used for downstream chemical conversion to other high-value products or can serve as microbial feedstocks (7, 20).

In acetogens, both formate and methanol enter the WLP within the methyl branch of the pathway. Formate is the first intermediate post-CO_2 fixation and therefore bypasses the gas assimilation step usually catalyzed by formate dehydrogenase (Fig. 1). Methanol is incorporated via the methanol-THF methyltransferase system to form methyl-THF, avoiding

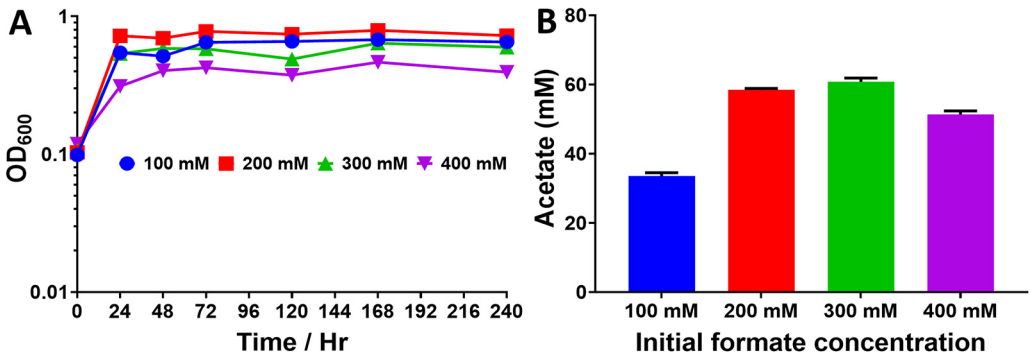

FIG 2 Formate tolerance of *B. methylotrophicum*. (A) Optical density throughout growth. (B) Final acetate concentrations after 240 h of growth. Error bars show standard errors of the means (SEM) for 3 biological replicates.

most of the metabolic cost in the form of ATP and NAD(P)H of the methyl branch (Fig. 1). In this instance, a three-part methyltransferase system is utilized, which first cleaves the C-O bond of methanol, using methyltransferase I (MTI), and transfers the methyl group to a corrinoid protein (CoP). The methyl group is then transferred from the methyl-CoP to THF creating methyl-THF by methyltransferase II (MTII) (21, 22).

Improving acetogenic conversion of both gaseous and liquid C_1 compounds is important in improving their viability in the circular carbon economy. *Butyribacterium methylotrophicum* is a methylotrophic acetogen studied most extensively throughout the 1980s to 1990s in an effort to elucidate its metabolism (23–28). Although distinct in name, the organism is considered a strain of *Eubacterium callanderi* KIST612 (formally *Eubacterium limosum* KIST612) due to their high genome sequence identity (99.7%) (29), so *B. methylotrophicum* will be referred to as "*B. methylotrophicum*." The organism gained attention due to its ability to grow on a variety of C_1 substrates (formate, methanol, CO, and CO_2) and its ability to produce both two-carbon (C_2) molecules such as acetate and ethanol alongside four-carbon (C_4) molecules including butyrate and butanol (23, 25–28) (Fig. 1). More recent studies have also developed a transformation protocol for this organism for future genetic engineering (30). A wide substrate and product range makes "*B. methylotrophicum*" an ideal candidate for converting C_1 substrates to high-value products, especially because the value of fatty acids increases substantially as more carbon is added to the chain (31, 32). The redox state within cells plays an integral role in determining product formation and modulation of products can therefore be achieved by varying the redox state of substrates (33, 34). For example, supplying more reduced substrates (CO or methanol) has the potential to shift the organism's metabolism to more reduced products (butyrate, ethanol, or butanol). This study explored "*B. methylotrophicum*" liquid and gas C_1 metabolism by adjusting substrate concentrations and feeding strategies and the employment of genetic engineering to improve C_4 product titers.

RESULTS

***B. methylotrophicum* tolerance to formate and methanol.** We first established tolerance of "*B. methylotrophicum*" to both formate and methanol by growing on increasing concentrations of each (up to 1 M) to determine if the organism could tolerate industrially viable concentrations. When grown on formate alone, the highest concentration at which growth was observed was 400 mM, with no detectable growth in concentrations above this (Fig. 2A). The highest observed optical density (OD) of ~0.75 was detected after 3 days of growth at 200 mM. Concentrations above this were inhibitory, with OD values decreasing as the concentration increased, suggesting formate toxicity above 200 mM. The methanol tolerance of "*B. methylotrophicum*" was unexpected, especially given the effects of formate, as "*B. methylotrophicum*" was able to grow on all concentrations of methanol tested (100 mM to 1,000 mM). The highest growth was seen in 100 mM methanol, reaching an OD of ~2 (Fig. 3A). Although all methanol concentrations tested showed growth, a successive decrease in OD was seen as the concentration of methanol was increased, suggesting that higher concentrations of methanol are tolerated but toxic to the bacterium. Although there

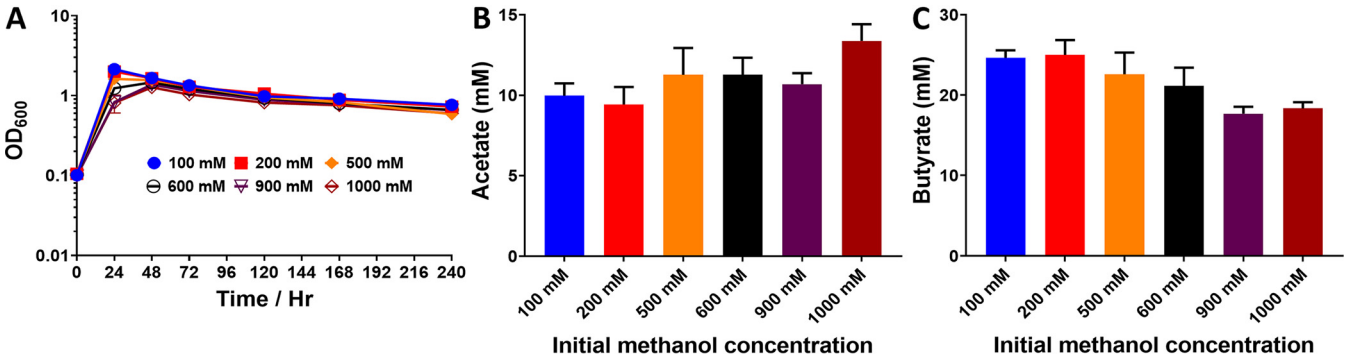

FIG 3 Methanol tolerance of *B. methylotrophicum*. (A) Optical density throughout growth. (B) Final acetate concentrations after 240 h of growth. (C) Final butyrate concentrations after 240 h of growth. Error bars show SEM for 3 biological replicates.

was evidence of methanol toxicity, methanol appears to serve as a better carbon source than formate for "*B. methylotrophicum*" due to the organism's ability to grow to ODs well over double that of formate alone.

Interestingly, growth on each of the sole substrates produced differing product profiles (Fig. 2 and 3). When grown on formate alone, "*B. methylotrophicum*" produced solely acetate, with the highest acetate concentrations observed reaching ~60 mM for both the 200 mM and 300 mM starting formate concentrations (Fig. 2B). In contrast, when grown on methanol alone, "*B. methylotrophicum*" produced butyrate as the major product, with concentrations reaching a maximum of ~25 mM with only ~14 mM acetate (Fig. 3B and C). Interestingly, although growth appeared to have stopped before either 24 or 48 h, depending on the initial methanol concentration, continued consumption of methanol and production of butyrate was seen, indicating that although growth may have ceased, methanol can still drive butyrate formation in vegetative cells (Fig. S2). We also observed that complete consumption of either formate (see Fig. S1A in the supplemental material) or methanol (Fig. S2A) was only observed for the 100 mM initial concentration for each, suggesting that either a limited amount of each substrate can be consumed or that another nutrient is limited when formate or methanol is the sole carbon source. Final carbon balance analysis also showed far higher carbon yield from methanol than from formate (Table S1).

Coutilization of formate and methanol enhances growth and increases C_4 product titers. To investigate whether "*B. methylotrophicum*" growth on C_1 compounds could be improved for maximal C_1 to C_4 conversion, we grew the organism on various initial ratios of mixed formate and methanol (Fig. 4). Most conditions improved "*B. methylotrophicum*" growth compared to growth solely on methanol or formate (Fig. 4A). Interestingly, we found significant increases in growth when there was a greater proportion of methanol than formate in the medium. The highest OD obtained was ~4 after 48 h of growth for ratios that exceed 2:1 (Fig. 4A). In contrast, when the methanol-to-formate ratio was lower, ODs of only ~2 were reached. Growth seemingly ended after 24 h, suggesting that it is the availability of excess methanol, and not formate, that drove growth improvements.

Unlike when formate was the sole carbon source, complete consumption of formate was seen for all concentrations tested (the majority consumed all formate by 24 h), indicating that the addition of methanol aided the utilization of formate (Fig. S3A). Complete, or nearly complete, consumption of methanol was only seen for cultures in which the initial methanol concentration was less than 200 mM (Fig. S3B). It was also clear that coconsumption of both substrates occurs. However, formate appears to be the preferred substrate, as it was consumed faster (Fig. S4A and B). Higher formate-to-methanol concentrations did, however, lead to lower final carbon yields, in keeping with formate or methanol as the sole substrate (Table S1).

Both acetate and butyrate were produced by all cultures. Excess formate drove acetate production, and high methanol-to-formate ratios favored butyrate production (Fig. 4B and C). Maximum butyrate concentrations reached ~45 mM (~4 g/liter) by the end of the experiment (Fig. 4C), far higher than any conditions tested previously (Fig. 3C). The observation that

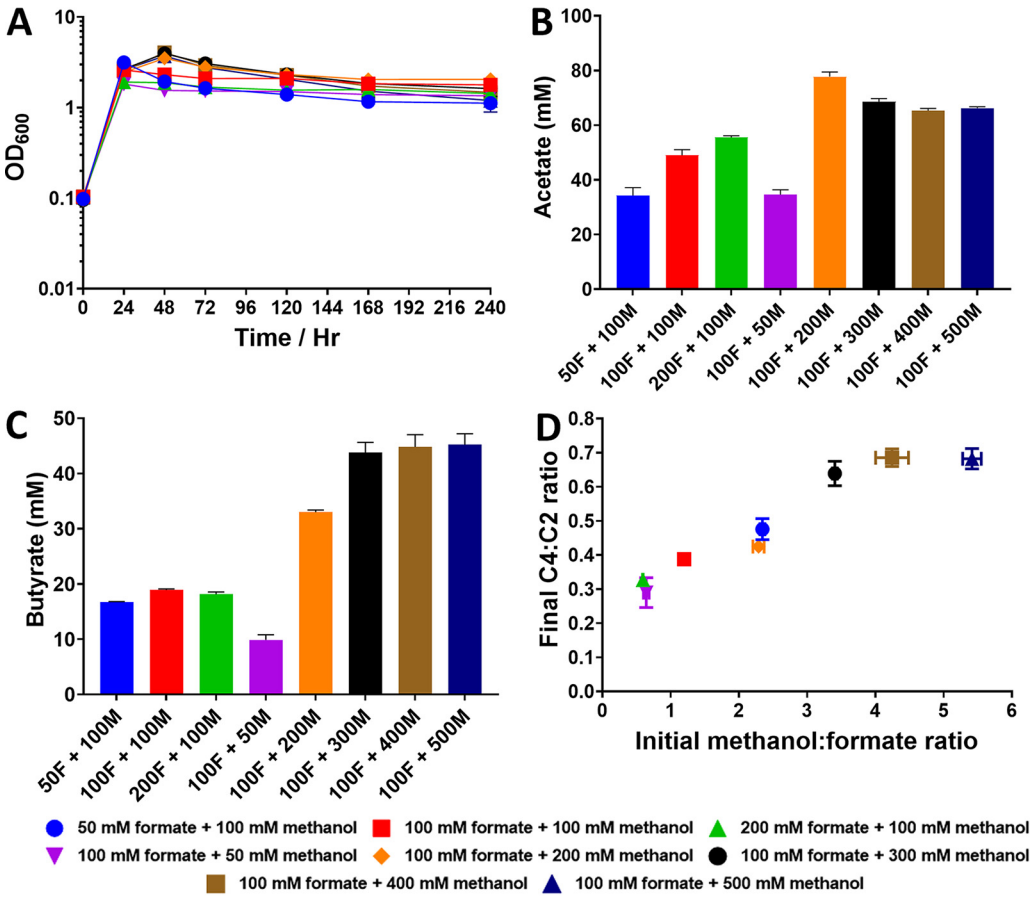

FIG 4 *B. methylotrophicum* growth and product profiles when grown with different methanol-formate ratios. (A) Optical density throughout growth. (B) Final acetate concentrations after 240 h of growth. (C) Final butyrate concentrations after 240 h of growth. (D) Final C_4:C_2 ratios compared to the initial methanol-formate ratio. Plotted methanol-formate ratios reflect exact substrate ratios measured by HPLC. Error bars show SEM for 3 biological replicates.

high methanol concentrations promote C_4 production was exemplified when we compared the initial methanol-formate ratios to the final C_4:C_2 (butyrate-acetate) ratios. A clear trend emerged showing that as the initial methanol-formate ratio was increased, the amount of C_4 products relative to C_2 products increased (Fig. 4D). Increasing C_4 production with excess methanol does, however, appear to be limited to methanol-formate ratios of up to 4:1 as both the 4:1 and 5:1 initial ratios produced comparable C_4:C_2 final ratios. The metabolism of "*B. methylotrophicum*" can clearly be altered by changing the ratios of substrates so that providing more reducing substrates like methanol pushes the metabolism to more reduced products such as butyrate.

Optimization of formate feeding strategies for improved C_4:C_2 ratios. As we discovered that "*B. methylotrophicum*" growth on methanol favors C_4 production but can be improved with the addition of formate, we sought to improve the C_4:C_2 ratios by testing three different formate feeding strategies, alongside providing excess methanol, within controlled fermenters. For each strategy tested, a total of 200 mM formate and 500 mM methanol was provided to the culture (Fig. 5A); 500 mM methanol was chosen, as although the 4:1 and 5:1 methanol-formate ratios produced similar C_4 titers, it was not known how formate delivery would affect the C_4:C_2 ratio, so methanol was provided at 500 mM so as not to be limiting. The first strategy entailed supplying all substrates to the cultures in our control reactor at the time of inoculation, which also served as a baseline for comparison. A second strategy employed a bolus feed in which 100 mM formate was added at the start of the fermentation, and then after consumption (~17 h) another 100 mM formate was added. We then employed a third feeding strategy in which 200 mM formate was slowly fed into

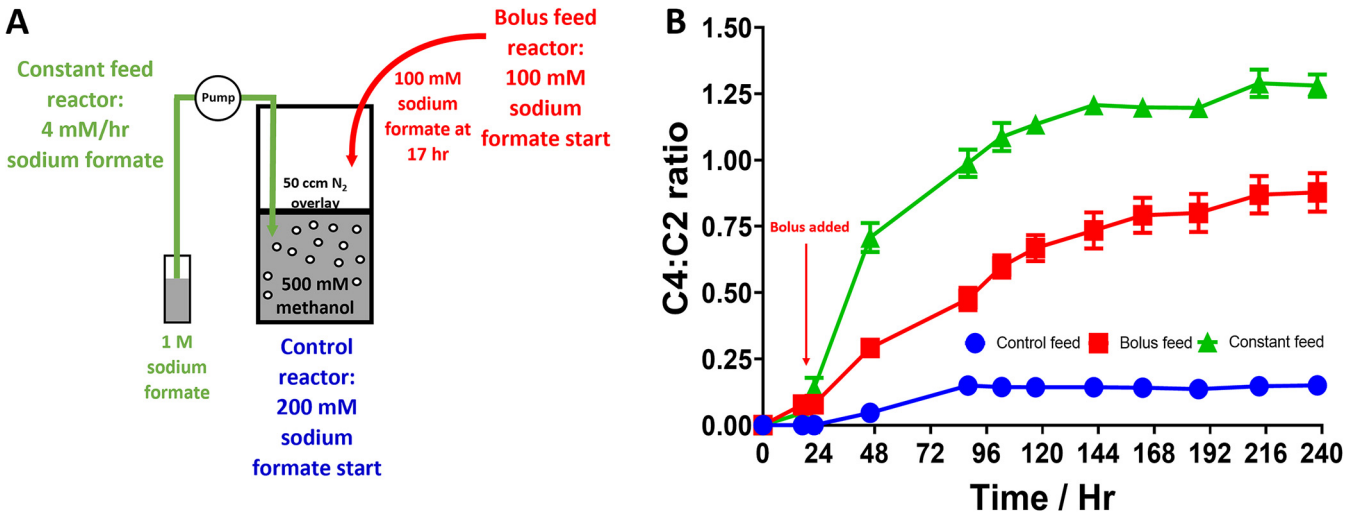

FIG 5 Bioreactor formate feeding strategies. (A) Schematic of the three fermentation setups used. (B) Ratios of C_4:C_2 products over time. Error bars show SEM for 3 biological replicates.

the bioreactor at a constant rate of 4 mM/h (Fig. 5A). The ratio of C_4:C_2 molecules was significantly increased when formate was added slowly in the constant feed reactor compared to when formate was added in bulk (Fig. 5B). C_4:C_2 ratios reached ~1.3 for the constant feed conditions compared to ~0.9 for the sequential bolus feed and ~0.15 for the control reactor after 240 h of growth. Methanol utilization also appeared to be enhanced for the constant feed, followed by the bolus feed and then the control (Fig. S4C). It should be noted that an abiotic fermentation was also carried out to measure methanol loss due to evaporation (data not shown). This fermentation showed losses of ~200 mM methanol and should be considered when measuring methanol utilization during these fermentations. Unlike methanol, formate was consumed for all conditions tested (Fig. S4B).

The addition of C_1 gases enhances the product spectrum of "*B. methylotrophicum*." As we established conditions under which "*B. methylotrophicum*" produced high titers of butyrate from formate and methanol, we wanted to observe whether the addition of C_1 gases would alter the "*B. methylotrophicum*" metabolism. Through adaptation, "*B. methylotrophicum*" has been shown to produce butanol from CO (26, 35); however, it is unclear whether the addition of formate and methanol alongside C_1 gases would improve "*B. methylotrophicum*" growth and product titers under our conditions. "*B. methylotrophicum*" was grown in pressurized bottles containing both gaseous and liquid C_1 substrates (Fig. 6). Growth on CO alone was limited, with the OD of the culture only reaching a maximum of ~0.2 (Fig. 6A), confirming the need for adaptation prior to growth on CO as the sole substrate. When methanol was provided alongside CO, growth was improved, with the OD of the culture reaching ~2 (Fig. 6A). This was also seen when CO_2 was supplied with methanol, which reached similar ODs (Fig. 6A). Growth with CO and formate did not produce substantial ODs, with the culture only appearing to grow after 168 h (Fig. 6A). When CO, formate, and methanol were supplied, growth was limited initially but did reach final ODs similar to those of CO plus methanol and CO_2 plus methanol (Fig. 6A). Growth with H_2 and methanol was limited and only reached an OD of ~0.35 (Fig. 6A). A decrease in bottle pressure, which indicates gas consumption, was seen for all conditions. However, the most substantial consumption was seen for the CO plus methanol, CO plus methanol plus formate, and CO_2 plus methanol conditions (Fig. 6B). We also observed the greatest methanol consumption from these conditions (Fig. 6D).

Most growth conditions produced acetate and/or butyrate (Fig. 6E and F). However, supplying both CO and methanol triggered butanol, ethanol, and lactate production (Fig. 6G, H, and I). Interestingly, lactate production was followed by a decrease in bottle pressure, suggesting that lactate acts as a temporary redox sink (Fig. 6I). Ethanol production preceded butanol (Fig. 6G), with butanol being detected only after 192 h of growth (Fig. 6H). The addition of more reduced substrates, such as CO, appeared to shift the "*B. methylotrophicum*"

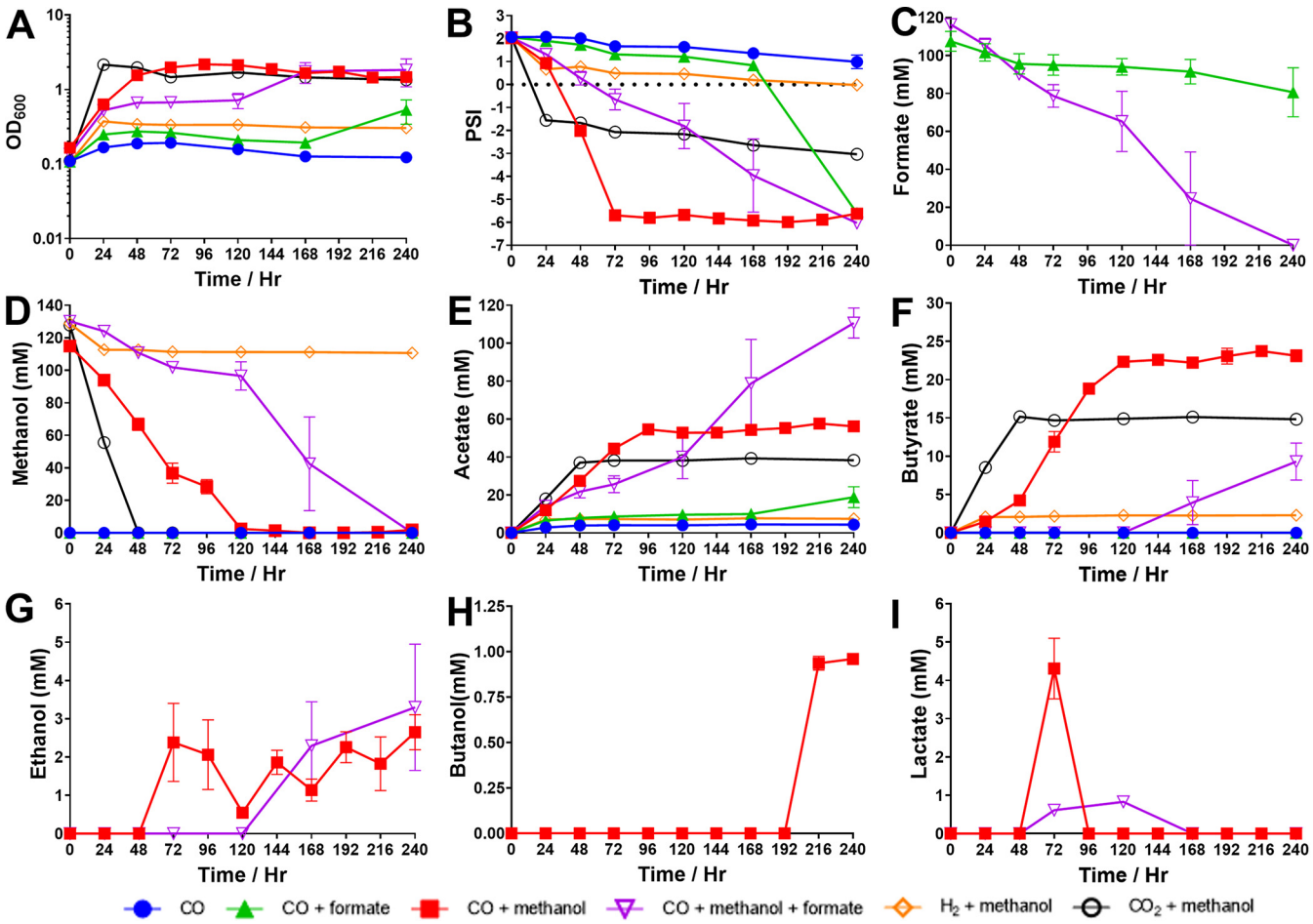

FIG 6 *B. methylotrophicum* fermentation profiles throughout mixotrophic C_1 gas and liquid growth. (A) Optical density throughout growth. (B) Bottle pressure throughout growth. (C) Formate concentration throughout growth. (D) Methanol concentration throughout growth. (E) Acetate concentration throughout growth. (F) Butyrate concentration throughout growth. (G) Ethanol concentration throughout growth. (H) Butanol concentration throughout growth. (I) Lactate concentration throughout growth. Error bars show SEM for 3 biological replicates.

metabolism toward more reduced products that could not be produced from formate or methanol alone or in combination. Furthermore, the addition of CO with methanol increased acetate production (Fig. 6E) compared to methanol alone (Fig. 3B), which we suspect is due to a greater availability of carbon for both branches of the WLP.

Development of a transformation protocol for "*B. methylotrophicum*." Although a transformation protocol was recently published for "*B. methylotrophicum*" (30), we developed our own method that requires no prior methylation of transformed plasmids and no cell-wall-weakening agents. Our transformation protocol is based on that of Leang et al. (36), with some modifications. In short, "*B. methylotrophicum*" was grown overnight in 200 mL of formate adapted medium (FAM) with 10 g/liter fructose and washed twice with SMP buffer (270 mM sucrose, 1 mM $MgCl_2$, and 7 mM sodium phosphate set to pH 6). Cells were then concentrated by resuspending in 1:200 (final volume-initial volume) SMP plus 10% dimethyl sulfoxide (DMSO) for electroporation. A full protocol for preparation of "*B. methylotrophicum*" electrocompetent cells and transformation can be found in Materials and Methods.

Due to their effectiveness as shuttle plasmids in clostridia, we tested transformation of plasmids from the pMTL80000 series (purchased from Chain Biotech, UK), which can carry a variety of different Gram-positive replicons for use in different organisms (37). We tested available Gram-positive replicons in the following plasmids: pMTL82151 (pBP1), pMTL83151 (pCB102), pMTL84151 (pCD6), and pMTL85151 (pIM13). We also tested pCL2 (pIP404), a derivative of pJIR750ai, that has worked well in the closely related species *Eubacterium callanderi* KIST612 and also in *Clostridium ljungdahlii* (36, 38). We did, however, adapt pCL2 by adding

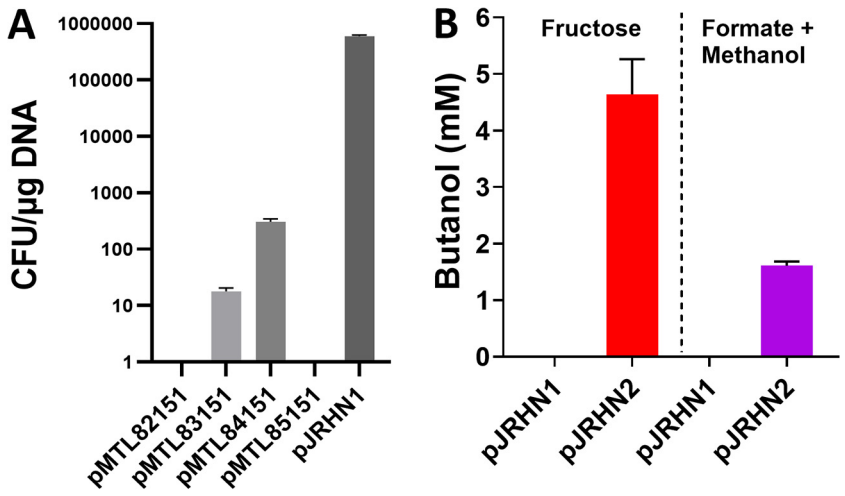

FIG 7 Transformation efficiencies and heterologous gene expression in *B. methylotrophicum*. (A) *B. methylotrophicum* transformation efficiency of tested plasmids. (B) Final butanol concentrations of pJRHN1 and pJRHN2 bearing strains during fructose and methanol plus formate growth. Error bars show SEM for 3 biological replicates.

the *lacZ* multiple cloning site derived from the pMTL vectors into pCL2. The newly created plasmid was named pJRHN1. We initially tested electroporation conditions similar to those of Leang et al. (36) and found that the most efficient electroporation conditions were 900 kV pulsing with resistance at 600 Ω and a capacitance of 25 μF using 25 μL cells in a 1-mm cuvette gap (detailed preparation and electroporation of "*B. methylotrophicum*" can be found in Materials and Methods). After transforming all previously mentioned vectors, colonies were only found for pMTL83151, pMTL84151, and pJRHN1, suggesting that pMTL82151 and pMTL85151 do not replicate in "*B. methylotrophicum*" using our transformation protocol (data not shown). We then tested transformation efficiencies for these three vectors by transforming 1 μg of plasmid DNA. We found that transformation efficiencies were the least for pMTL83151 at 18 $\pm$ 2.5 CFU/μg DNA, followed by pMTL84151 at 305 $\pm$ 38 CFU/μg DNA (Fig. 7A). Electroporation of pJRHN1 produced significantly higher CFU counts than the other two plasmids tested, giving a transformation efficiency of $6.0 \times 10^5 \pm 3.0 \times 10^4$ CFU/μg DNA (Fig. 7A). Transformation of "*B. methylotrophicum*" was confirmed by thiamphenicol resistance and PCR verification using primers targeting the plasmid-borne *catP* gene. Wild-type "*B. methylotrophicum*" genomic DNA and water were used as negative controls (Fig. S5).

Heterologous gene expression of the *C. acetobutylicum adhE2* gene in "*B. methylotrophicum*" increases butanol production. With an effective transformation protocol developed, we wanted to see if heterologous gene expression using pJRHN1 in "*B. methylotrophicum*" was possible. Under our conditions, "*B. methylotrophicum*" butanol production was limited to growth with CO plus methanol, even though the organism possesses several alcohol dehydrogenase (*adhE*) genes (BUME_03560, BUME_11170, BUME_24570, BUME_02770, and BUME_22490). The *adhE2* gene of *C. acetobutylicum* (CA_P0035), however, is known to be directly involved in butanol formation, catalyzing the conversion of butyryl-CoA to butanol (39). We subsequently constructed the plasmid pJRHN2, which contained the *adhE2* gene of *C. acetobutylicum* under the control of the desulfoferrodoxin gene's (BUME_12740) supposed promoter (Pdfx). This promoter was shown to provide high levels of transcription in the related *E. callanderi* KIST612 (38). Once gene sequences were confirmed, pJRHN2 was transformed into "*B. methylotrophicum*," and successful transformants were selected for by growth in the presence of thiamphenicol. pJRHN2-bearing strains were grown for 5 days in FAM with either 10 g/liter fructose or 100 mM formate plus 100 mM methanol to test gene expression under heterotrophic sugar and liquid C_1 conditions, respectively. "*B. methylotrophicum*" harboring pJRHN1 was grown under the same conditions as a control.

Butanol was detected by all strains carrying pJRHN2, which reached ~5 mM and ~1.5 mM after 5 days of growth under sugar and liquid C_1 conditions, respectively (Fig. 7B). Ethanol was also detected from pJRHN2-harboring strains when grown in fructose but not

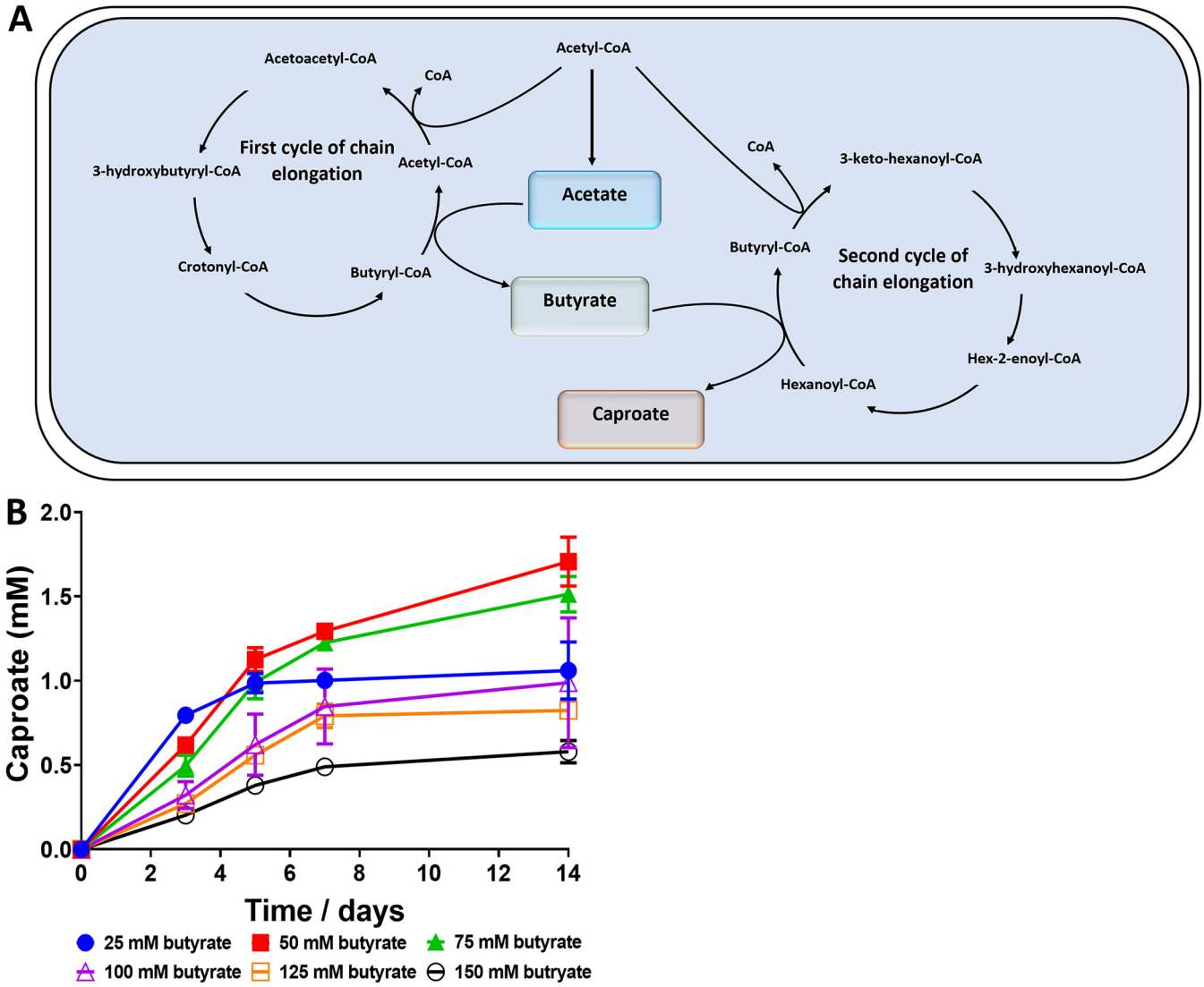

FIG 8 Evidence of chain elongation by *B. methylotrophicum*. (A) Schematic of chain elongation to six-carbon molecules. (B) Caproate concentration over time. Error bars show SEM for 3 biological replicates.

when grown with formate plus methanol (Fig. S7G). No alcohols were detected from the strain carrying pJRHN1 under these conditions. Acetate and butyrate were produced by all plasmid-bearing strains (Fig. S7D and E). Lactic acid was detected by plasmid-bearing strains grown on fructose but not on formate plus methanol (Fig. S7F). Optimization is required to improve alcohol production; however, the presence of *adhE2* on pJRHN2 allowed for butanol production, showing that heterologous gene expression is possible in "*B. methylotrophicum*."

Evidence of further chain elongation by "*B. methylotrophicum*." *Clostridium kluyveri* is capable of fermenting ethanol and acetate to longer-chained molecules (C_6+) using a metabolic pathway similar that of "*B. methylotrophicum*" to produce butyrate (40). Furthermore, other acetogens, such as *Clostridium carboxidivorans*, have been shown to make C_6 molecules from syngas (41). The extension of the carbon chain is via iterative cycles of the reverse β-oxidation pathway to add acetyl-groups at each cycle to the growing chain (Fig. 8A). Caproate (C_6) is a product of great interest, as it can be efficiently converted to diesel and aviation fuel replacements (42). Furthermore, it has also been shown that methanol can drive chain elongation in *E. limosum* (43). We therefore aimed to observe whether "*B. methylotrophicum*" could also produce caproate (C_6) when provided with excess methanol and butyrate. We supplied "*B. methylotrophicum*" with 500 mM methanol and 25 mM to 150 mM butyrate to observe if increasing the butyrate concentration increased C_6 production.

Samples were taken 1 week postinoculation. Production of caproate was seen for all conditions tested (Fig. 8B), with a maximum caproate concentration of ~1.7 mM observed when "*B. methylotrophicum*" was supplied with 50 mM butyrate. Acetate was produced by all cultures (Fig. S8B) alongside small increases in butyrate (Fig. S8C). We suspect the increase in butyrate is due to the organism metabolizing methanol into butyrate while simultaneously producing caproate. As a proof of principle, the production of caproate provides circumstantial evidence that "*B. methylotrophicum*" is capable of chain elongation to higher-value products (C_6), but this requires further investigation and optimization.

DISCUSSION

"*B. methylotrophicum*" can utilize a wide variety of C_1 substrates, making it an interesting candidate for C_1-to-product conversion (23–28, 35, 44–46). The organism showed a high tolerance to both formate and methanol, as it could grow in up to 400 mM formate and 1,000 mM methanol, which is higher than what has been reported for other acetogens (7). The highest reported acetogen growth on methanol has been 900 mM by *Acetobacterium woodii*, which, as with "*B. methylotrophicum*," showed growth defects as the methanol concentration was increased (22). Concentrations of methanol above 1,000 mM therefore were not tested due to the reports for *A. woodii*. Although increasing concentrations of methanol did decrease "*B. methylotrophicum*" growth, growth was not abolished at 1,000 mM, so it can be assumed that the organism could grow at a concentration higher than 1,000 mM methanol. Tolerance to high concentrations of formate and methanol can be reached by acetogens, unlike aerobic fermentation, as formate does not inhibit cytochrome *c* oxidases and toxic formaldehyde is not formed from methanol (7, 47, 48).

The different carbon sources influenced the product spectrum of "*B. methylotrophicum*." Our data show that formate utilization favors acetate production and methanol utilization favors butyrate production. No butyrate was detected on growth solely on formate, whereas butyrate was the major, though not only, product of methanol fermentation (Fig. 2 and 3). The difference in products is likely due to their different entry points into the WLP (Fig. 1). Formation of acetyl-CoA from C_1 compounds requires input from both the carbonyl and methyl branches within the WLP (9). Growth on either substrate will require sections of the methyl branch to be run in the reverse direction to supply CO_2 necessary for the carbonyl branch. Growth on formate through the carbonyl branch, after conversion to CO_2, is redox balanced as the reduced cofactor gained from formate oxidation is used for CO_2 reduction. However, an investment of one ATP and two NADH equivalents is required for formate to traverse the methyl branch of the WLP (Fig. 1). Acetate is likely the preferred product in formate-fed growth, as investment of one ATP is recuperated through substrate-level phosphorylation without requiring additional reducing equivalents. As this process is net zero ATP, additional ATP is generated by the Rnf (*Rhodobacter* nitrogen fixation) complex, which exports sodium or H^+ ions for subsequent use by the ATP synthase for ATP generation (Fig. 1) (49). In contrast, methanol as the starting substrate requires no investment in the forward direction of the methyl branch as it enters directly as methyl-THF via the use of the methyltransferase system (Fig. 1) (21). Reversal of the methyl branch at this stage results in a net gain of one ATP and two NADH equivalents when generating CO_2 for the carbonyl branch. The additional NADH generated in methanol oxidation obligated NAD^+ regenerating reactions for redox balance, which drives butyrate formation by the NADH-dependent 3-hydroxybutyryl-CoA dehydrogenase (Hbd) and butyryl-CoA dehydrogenase (Bcd) enzymes (Fig. 1). Therefore, the lack of butyrate production under formate-fed conditions can be explained by the lack of available reducing equivalents. Furthermore, growth on methanol has been calculated to produce 1.83 ATP/butyrate (21), more than when grown on formate, thus explaining why butyrate is favored in the presence of methanol, as methanol provides NADH and more ATP (13, 21).

Mixotrophic growth of both formate and methanol significantly enhanced "*B. methylotrophicum*" growth and C_4 titers, especially when methanol was in excess to formate. As seen from Fig. 4D, increasing the initial ratio of methanol to formate caused an increase in the ratio of C_4 to C_2. Butyrate production reached a maximum of ~45 mM (~4 g/liter), far higher than recently reported *E. limosum* growth on methanol and more recent "*B. methylotrophicum*"

studies on methanol and bicarbonate (both ~25 mM butyrate) (13, 30). It is evident that although formate utilization does not favor butyrate production, reaching higher C_4 titers requires both substrates in ratios where methanol is in excess to formate. With this in mind, we chose not to test formate concentrations higher than 200 mM to avoid shifting the metabolism toward acetate production. Under mixed substrate conditions, we speculate that formate is converted to CO_2, reduced to CO (using reduced ferredoxin) by the CODH/ACS, and combined with the methyl group from methanol. This would provide the necessary components needed for acetyl-CoA synthesis without the costly metabolic requirement of the methyl branch of the WLP. Acetate is then produced for ATP generation for the cell. This hypothesis, however, lacks generation of the required NADH for both butyrate production and reduced ferredoxin to reduce CO_2 to CO (assuming reduced ferredoxin is not gained from formate oxidation). Therefore, to balance the redox within the cell, methanol is also oxidized to generate NADH alongside direct conversion to methyl-THF. Generated NADH is then used by the 3-hydroxybutyrl-CoA dehydrogenase (Hbd) and butyryl-CoA dehydrogenase (Bcd)-electron-transferring flavoprotein (Etf) complex, which, in the case of the Bcd-Etf complex, also produces reduced ferredoxin required for CO_2 reduction (49). Butyrate production therefore serves not as an ATP-generating step but as a reduced-ferredoxin-generating step, and production of acetate drives ATP generation along with the *Rnf* complex.

We have shown that growth on methanol and butyrate titers could be improved by the addition of formate. Furthermore, we showed that the timing of formate delivery impacted C_4 titers. By slowly feeding formate into the bioreactor, compared to being added completely at the start or as a bolus feed, we were able to improve the ratios of C_4:C_2 products (Fig. 5B). Low concentrations of formate in this strategy provided enough conversion to CO_2, and then reduction to CO, without significantly shifting the metabolism away from C_4 production. With excess methanol provided alongside, we speculate that "*B. methylotrophicum*" was forced to grow predominantly on methanol, which favors butyrate production, but was provided with the necessary CO_2 for the CODH/ACS from the limited formate. This allowed for sustained high butyrate production over acetate, further improving the yields of the more desired product. Adjusting the feeding strategies is another example of how it is possible to modulate "*B. methylotrophicum*" product profiles through providing different concentrations of substrates.

We also showed, as a proof of principle, that "*B. methylotrophicum*" can elongate carbon molecules further and produce caproate (C_6) (Fig. 8). *C. kluyveri* utilizes cycles of the reverse β-oxidation pathway to add carbon onto the chain using ethanol and acetate as initial substrates (40). Because "*B. methylotrophicum*" uses this pathway to produce butyrate, we hypothesized that the organism can produce caproate when supplied with excess methanol and butyrate. This hypothesis was confirmed, as production of caproate was seen for all conditions tested (Fig. 8).

"*B. methylotrophicum*" has been shown to produce lactate under syngas conditions (45). However, when we supplied methanol and CO, lactate concentrations were increased to ~4 mM compared ~1 mM from previous studies (45). Lactate is an important product in the pharmaceutical and food industry, alongside industrial production of biodegradable plastics (50). Lactate is produced through two reactions, first via the pyruvate-ferredoxin oxidoreductase (PFOR), which catalyzes the reversible conversion of acetyl-CoA to pyruvate using CO_2 and reduced ferredoxin (8, 51). From here, the lactate dehydrogenase (Ldh) reversibly converts pyruvate to lactate with NADH, which, if completed by an electron-bifurcating Ldh, can yield reduced ferredoxin (50, 52). However, it is unclear whether the Ldh from "*B. methylotrophicum*" is electron bifurcating. We hypothesize that large quantities of relatively reduced substrates (CO and methanol) caused lactate production due to higher ratios of reduced ferredoxin/oxidized ferredoxin and NAD(P)H/NAD(P)$^+$ within the cell. The CODH can reversibly convert CO to CO_2 reducing ferredoxin, and, as mentioned, reversal of the methyl branch of the WLP through methanol utilization yields NADH. Transient production of certain products has been reported several times in acetogens and appears to be linked to the redox state of the cell (33, 34). As lactate production occurred when the decrease in bottle pressure reached its peak (Fig. 6B), we hypothesize that lactate served as a redox sink to balance the elevated quantities

TABLE 1 Strains and plasmids used in this study

Strain or plasmid	Feature	Source or reference
Strain		
Escherichia coli NEB 5-alpha	Cloning strain	NEB
Clostridium acetobutylicum ATCC 824	Wild type *C. acetobutylicum* ATCC 824	ATCC
Butyribacterium methylotrophicum DSM 3468	Wild type *B. methylotrophicum*	ATCC
B. methylotrophicum with pJRHN1	*B. methylotrophicum* harboring pJRHN1	This study
B. methylotrophicum with pJRHN2	*B. methylotrophicum* harboring pJRHN2	This study
Plasmid		
pMTL83151	Modular plasmid of the pMTL series	Chain Biotech, 37
pCL2	Modified pJIR750ai	36
pJRHN1	pCL2 containing the *lacZ* module	This study
pJRHN2	pJRHN1 contain the *dfx* promoter and *adhE2* gene	This study

of reduced ferredoxin and NADH, which we suspect reached its maximum at 72 h. Consumption of lactate followed, suggesting the lack of CO after 72 h allowed the organism to reassimilate the lactate. Similarly, alcohols, which require 2 NAD(P)H equivalents, were also produced under this condition, which we assume is due to an increase in reduced equivalents in the cell. The redox state of substrates plays an important role in product formation.

Improving product titers through genetic engineering is another important tool in improving acetogen viability in the bioeconomy (53). We showed successful heterologous gene expression of the *adhE2* gene from *C. acetobutylicum* that leads to butanol production under conditions where butanol was not usually detected (Fig. 7B). Both genetic engineering and substrate selection are important tools and may serve in conjunction for improved product titers. Additionally, the butyrate/butanol pathway (Fig. 1) shares many common enzymatic steps with other pathways investigated for the production of value-added products, such as (poly)hydroxyalkanoates, by acetogens (54, 55). As far as we know, acetogen conversion of liquid C_1 substrates to these products has not been explored but could be a promising avenue of research. Using "*B. methylotrophicum*," we show that acetogen metabolism can be modified through substrate selection, feeding, and genetic engineering to further unlock their industrial potential for biological carbon capture.

MATERIALS AND METHODS

Bacterial strains and growth conditions. "*B. methylotrophicum*" DSM 3468 was purchased from the German Collection of Microorganisms and Cell Cultures (DSMZ) and cultivated under strict anaerobic conditions in an adapted version of ATCC medium 1136, named formate-adapted medium (FAM) (Table 1). FAM contains (per liter) 20 mL of 3 M potassium phosphate buffer that contained 321.5 g/liter K_2HPO_4 and 157.2 g/liter KH_2PO_4, 50 mL mineral solution 2 that contains 6 g/liter $(NH_4)_2SO_4$, 12 g/liter NaCl, 2.4 g/liter $MgSO_4 \cdot 7H_2O$, and 1.6 g/liter $CaCl_2 \cdot 2H_2O$, 50 mL sodium carbonate solution that contains 80 g/liter Na_2CO_3, 1 g/liter yeast extract, 0.6 g/liter L-cysteine HCl, 10 mL trace element solution, and 10 mL Wolfe's vitamin solution. Trace element solution and Wolfe's vitamin solution are identical to those found in ATCC medium 1754 PETC. The medium was prepared and the pH adjusted to 7.2, and then it was filter sterilized. For growth on agar plates and recovery posttransformation, YTF medium was used that contained 10 g/liter yeast extract, 16 g/liter Bacto tryptone, 4 g/liter NaCl, 5 g fructose, 0.5 g/liter L-cysteine HCl set to pH 7. The addition of 15 g/liter Bacto agar was used for solid plates. "*B. methylotrophicum*" growth was examined in a COY (Grass Lake, MI) anaerobic growth chamber, flushed with 95% N_2 and 5% H_2 and maintained anaerobic by palladium catalyst or in pressurized bottles.

For the formate and methanol tolerance and mixed formate and methanol ratio experiments, "*B. methylotrophicum*" growth was carried out in 15-mL Falcon tubes (Fisher Scientific) using 10 mL FAM and various formate and methanol concentrations at 37°C. For caproate production, "*B. methylotrophicum*" growth was carried out in 15-mL Falcon tubes (Fisher Scientific) using 5 mL FAM, 500 mM methanol, and various butyrate concentrations at 37°C. Growth for the plasmid-bearing strains was carried out in 15-mL Falcon tubes (Fisher Scientific) using 10 mL FAM with either 10 g/liter fructose or 100 mM formate and 100 mM methanol and supplemented with 10 μg/ml thiamphenicol at 37°C. Growth with CO, CO_2, or H_2 supplementation was carried out using 250 mL Duran Pressure Plus bottles (DWK Life Sciences, USA) containing 50 mL FAM and various formate and methanol concentrations. Bottles were sealed and aseptically flushed with either CO, CO_2, or H_2 for 3 min depending on the required gas. CO, CO_2, or H_2 was then added to the required pressure. FAM within the bottles was supplemented with 10 μg/mL thiamphenicol for growth with plasmid-bearing strains. Bottle growth was carried out at 37°C with 200-rpm shaking.

Escherichia coli NEB 5-alpha was used for all plasmid preparations and was acquired from New England Biolabs (NEB). NEB 5-alpha was grown in LB medium at 37°C using 30 μg/mL chloramphenicol to maintain plasmid selection.

TABLE 2 Primers used in this study

Primer name	Sequence (5′–3′)	Description	Source
cl2hifi_fwd	GGGTTACATCGAACTGGATC	Amplification of pCL2	This study
cl2hifi_rev	CCACAGAATCAGGGGATAAC	Amplification of pCL2	This study
laczhifi_fwd	GTTATCCCCTGATTCTGTGGCCTGCAGGATAAAAAAATTGTAG	Amplification of LacZ multiple cloning site	This study
laczhifi_rev	GATCCAGTTCGATGTAACCCGGCGCGCCATAAAAATAAG	Amplification of LacZ multiple cloning site	This study
Pdfx_fwd	GCTCGGTACCCGGGGATCCTTATAATTATTTAAAATATCAACAGACATCTC	Amplification of *dfx* promoter	This study
Pdfx_rev	TAACTTTCATAATAAAGACCTCCTATAGTCC	Amplification of *dfx* promoter	This study
Cac adhE2_fwd	GGTCTTTATTATGAAAGTTACAAATCAAAAAGAAC	Amplification of *C. acetobutylicum adhE2* gene	This study
Cac adhE2_rev	ATGGACGCGTGACGTCGACTTTAAAATGATTTTATATAGATATCCTTAAGTTC	Amplification of *C. acetobutylicum adhE2* gene	This study
catP_F	CCGGCCAGTGGGCAAGTTGAAAAATTC	Amplification of the *catP* gene	This study
catP_R	AAACTTAGGGTAACAAAAAACACCGTATT	Amplification of the *catP* gene	This study

Bioreactor conditions. For testing formate-feeding strategies, "*B. methylotrophicum*" was grown in Biostat Q plus 0.5-liter bioreactors (Sartorius Stedim) with a 300-mL initial working volume of FAM with 500 mM methanol. A total of 200 mM formate was supplied through three distributions. The first was a control bioreactor setup that contained 200 mM formate at the start of growth with no added formate during growth. The second bioreactor setup contained 100 mM formate at the start of growth and cultures subsequently given a bolus feed of 100 mM formate at 17 h. The third bioreactor setup contained no starting formate; however, cultures were supplied a constant feed of formate after inoculation at 4 mM/h, from a 1 M sodium formate stock, for the first 50 h. Each condition was in biological triplicate, and samples were taken for the optical density at 600 nm (OD_{600}) and high-performance liquid chromatography (HPLC) at least once a day for 10 days. Fermentation conditions were carried out at 37°C, with 200-rpm stirring. An overlay of 50 ccm of N_2 was applied continuously throughout the experiment. The pH of all bioreactor growths was held at 7 using 2 M HCl.

Molecular techniques. Plasmids from the pMTL80000 modular system (37) were purchased from Chain Biotech (Nottingham, UK) and used for testing transformation in "*B. methylotrophicum*." Plasmid pCL2 was obtained by following the same modifications that Leang et al. performed after purchasing pJIR750ai from Sigma (36). Plasmid pJRHN1 was made by placing the *lacZ*α multiple-cloning site module from pMTL84151 into pCL2 using the NEBuilder HiFi DNA assembly cloning kit (NEB). Both the pCL2 fragment and *lacZ*α multiple-cloning site module from pMTL84151 were amplified using Phusion polymerase (NEB) and primers listed in Table 2. Plasmid pJRHN2 for heterologous gene expression of the *adhE2* gene from *Clostridium acetobutylicum* ATCC 824 was constructed by insertion of both the 200-bp sequence upstream on the "*B. methylotrophicum*" desulfoferrodoxin (BUME_12740) gene and the *adhE2* gene of *C. acetobutylicum* into pJRHN1. Fragments were amplified using Phusion polymerase (NEB) and inserted at the XbaI (NEB) cut site. *C. acetobutylicum* and "*B. methylotrophicum*" genomic DNA was isolated using a GenElute bacterial genomic DNA kit (Sigma-Aldrich, USA) by following the manufacturer's instructions and used as a template for the primers listed in Table 2. *E. coli* transformants were screened by colony PCR using DreamTaq (ThermoFisher Scientific). Plasmids were isolated using a Monarch plasmid miniprep kit (NEB) by following the manufacturer's instructions, and insertions were verified by Sanger sequencing (Genewiz). Plasmid maps of pJRHN1 and pJRHN2 can be found in the supplemental material (Fig. S3).

Preparation of electrocompetent cells and plasmid transformation into "*B. methylotrophicum*." "*B. methylotrophicum*" was grown in 200 mL of FAM containing 10 g/liter fructose overnight at 37°C. The OD_{600} for harvesting at this time point was ~3.5. Cells were then centrifuged at 4,000 × *g* for 15 min at 4°C. Cells were then washed and resuspended in 100 mL ice-cold SMP buffer (270 mM sucrose, 1 mM $MgCl_2$, and 7 mM sodium phosphate set to pH 6). Centrifugation and resuspension steps were repeated once more. A final centrifugation step was then completed. The resulting cell pellet was resuspended in 1 mL SMP buffer plus 10% DMSO. Cells were divided into 200-μL aliquots in sterile microcentrifuge tubes and frozen at −80°C for future use.

Electroporation was performed in a COY chamber with a Bio-Rad (Hercules, California) Gene Pulser Xcell electroporator under the following conditions: 25 μL cells was mixed with 1 to 2 μg of DNA in a 1-mm electroporation cuvette, pulsed at 900 kV with resistance at 600 Ω and a capacitance of 25 μF. Cells were then resuspended in 1 mL of YTF and recovered for 8 to 16 h at 37°C. Cells were then plated in anaerobic molten YTF agar with thiamphenicol at a final concentration of 10 μg/mL. Typically, colonies appeared between 2 and 5 days after plating.

Analytical techniques. Samples of cultures were routinely analyzed for cell density and concentrations of substrates and products via HPLC. Samples (1 mL) were taken at various time points and optical density was measured at 600 nm using a Milton Roy (Ivyland, PA) Spectronic 21D. Dilutions were made as necessary to keep readings within the dynamic range of the instrument. HPLC samples were prepared from undiluted samples by pelleting the cells by centrifugation at full speed for 1 min and then filtering the supernatant through a 0.22-μm filter. Fermentation substrates and products in the liquid phase (fructose, formate, acetate, methanol, ethanol, butyrate, caproate, and butanol) were measured by HPLC on a 1200 series Agilent (Santa Clara, CA) with an Aminex HPX-87H column using a Micro Guard Cation H cartridge at 55°C with 4 mM H_2SO_4 mobile phase, as previously described (56).

Carbon and electron yield calculations. Carbon yield was calculated based on total carbon concentration of the final products divided by the carbon concentration of liquid C_1 substrates used. Carbon concentration for products was determined by the number of carbons in the molecule, for example, each acetate contains 2 carbon molecules, so 10 mM acetate would have 20 mM carbon. Electron yield was calculated based on the degree of reduction, defined as the number of equivalents of available electrons each substrate or product has. Thus, the electron yield can be calculated by the number of available electrons as

products divided by the number of electrons as substrates. As only liquid substrates and products are assessed, CO_2 and H_2 are not accounted for in the calculations.

SUPPLEMENTAL MATERIAL

Supplemental material is available online only.

SUPPLEMENTAL FILE 1, PDF file, 0.9 MB.

ACKNOWLEDGMENTS

We thank Katherine Chou for her editing of the manuscript.

This work was authored by the National Renewable Energy Laboratory, operated by Alliance for Sustainable Energy, LLC, for the U.S. Department of Energy (DOE) under contract no. DE-AC36-08GO28308. Funding was provided by DOE and Bioenergy Technology Office (BETO). The views expressed in the article do not necessarily represent the views of the DOE or the U.S. Government. The U.S. Government retains and the publisher, by accepting the article for publication, acknowledges that the U.S. Government retains a nonexclusive, paid-up, irrevocable, worldwide license to publish or reproduce the published form of this work, or allow others to do so, for U.S. Government purposes.

J.R.H., H.R., L.M., Y.P., and J.L. designed the research; J.R.H., S.D.H., H.R., L.M., C.U., and Y.P. performed the research; and J.R.H., S.D.H., and J.L. wrote the manuscript.

We declare no conflict of interest.

REFERENCES

1. Satanowski A, Bar-Even A. 2020. A one-carbon path for fixing CO_2. EMBO Rep 21:e50273. https://doi.org/10.15252/embr.202050273.
2. Lee RP, Keller F, Meyer B. 2017. A concept to support the transformation from a linear to circular carbon economy: net zero emissions, resource efficiency and conservation through a coupling of the energy, chemical and waste management sectors. Clean Energy 1:102–113. https://doi.org/10.1093/ce/zkx004.
3. Grim RG, Huang Z, Guarnieri MT, Ferrell JR, Tao L, Schaidle JA. 2020. Transforming the carbon economy: challenges and opportunities in the convergence of low-cost electricity and reductive CO_2 utilization. Energy Environ Sci 13:472–494. https://doi.org/10.1039/C9EE02410G.
4. Álvarez A, Bansode A, Urakawa A, Bavykina AV, Wezendonk TA, Makkee M, Gascon J, Kapteijn F. 2017. Challenges in the greener production of formates/formic acid, methanol, and DME by heterogeneously catalyzed CO_2 hydrogenation processes. Chem Rev 117:9804–9838. https://doi.org/10.1021/acs.chemrev.6b00816.
5. Kätelhön A, Meys R, Deutz S, Suh S, Bardow A. 2019. Climate change mitigation potential of carbon capture and utilization in the chemical industry. Proc Natl Acad Sci U S A 116:11187–11194. https://doi.org/10.1073/pnas.1821029116.
6. Müller V. 2019. New horizons in acetogenic conversion of one-carbon substrates and biological hydrogen storage. Trends Biotechnol 37:1344–1354. https://doi.org/10.1016/j.tibtech.2019.05.008.
7. Cotton CA, Claassens NJ, Benito-Vaquerizo S, Bar-Even A. 2020. Renewable methanol and formate as microbial feedstocks. Curr Opin Biotechnol 62:168–180. https://doi.org/10.1016/j.copbio.2019.10.002.
8. Ragsdale SW. 2008. Enzymology of the Wood-Ljungdahl pathway of acetogenesis. Ann N Y Acad Sci 1125:129–136. https://doi.org/10.1196/annals.1419.015.
9. Schuchmann K, Müller V. 2014. Autotrophy at the thermodynamic limit of life: a model for energy conservation in acetogenic bacteria. Nat Rev Microbiol 12:809–821. https://doi.org/10.1038/nrmicro3365.
10. Müller V. 2003. Energy conservation in acetogenic bacteria. Appl Environ Microbiol 69:6345–6353. https://doi.org/10.1128/AEM.69.11.6345-6353.2003.
11. Ragsdale SW, Pierce E. 2008. Acetogenesis and the Wood-Ljungdahl pathway of CO_2 fixation. Biochim Biophys Acta 1784:1873–1898. https://doi.org/10.1016/j.bbapap.2008.08.012.
12. Litty D, Müller V. 2021. Butyrate production in the acetogen Eubacterium limosum is dependent on the carbon and energy source. Microb Biotechnol 14:2686–2692. https://doi.org/10.1111/1751-7915.13779.
13. Flaiz M, Ludwig G, Bengelsdorf FR, Dürre P. 2021. Production of the biocommodities butanol and acetone from methanol with fluorescent FAST-tagged proteins using metabolically engineered strains of *Eubacterium limosum*. Biotechnol Biofuels 14:117. https://doi.org/10.1186/s13068-021-01966-2.
14. Rabinowitz JA, Kanan MW. 2020. The future of low-temperature carbon dioxide electrolysis depends on solving one basic problem. Nat Commun 11:1–3. https://doi.org/10.1038/s41467-020-19135-8.
15. Jhong HRM, Ma S, Kenis PJ. 2013. Electrochemical conversion of CO_2 to useful chemicals: current status, remaining challenges, and future opportunities. Curr Opin Chem Eng 2:191–199. https://doi.org/10.1016/j.coche.2013.03.005.
16. Yishai O, Lindner SN, Gonzalez de la Cruz J, Tenenboim H, Bar-Even A. 2016. The formate bio-economy. Curr Opin Chem Biol 35:1–9. https://doi.org/10.1016/j.cbpa.2016.07.005.
17. Petrognani C, Boon N, Ganigué R. 2020. Production of isobutyric acid from methanol by: *Clostridium luticellarii*. Green Chem 22:8389–8402. https://doi.org/10.1039/D0GC02700F.
18. Szima S, Cormos CC. 2018. Improving methanol synthesis from carbon-free H_2 and captured CO_2: a techno-economic and environmental evaluation. J CO2 Util 24:555–563. https://doi.org/10.1016/j.jcou.2018.02.007.
19. Methanol Institute Renewable Methanol. Renewable methanol. www.methanol.org. Accessed 5 November 2021.
20. Schrader J, Schilling M, Holtmann D, Sell D, Filho MV, Marx A, Vorholt JA. 2009. Methanol-based industrial biotechnology: current status and future perspectives of methylotrophic bacteria. Trends Biotechnol 27:107–115. https://doi.org/10.1016/j.tibtech.2008.10.009.
21. Kremp F, Müller V. 2021. Methanol and methyl group conversion in acetogenic bacteria: biochemistry, physiology and application. FEMS Microbiol Rev 45:fuaa040. https://doi.org/10.1093/femsre/fuaa040.
22. Kremp F, Poehlein A, Daniel R, Müller V. 2018. Methanol metabolism in the acetogenic bacterium *Acetobacterium woodii*. Environ Microbiol 20:4369–4384. https://doi.org/10.1111/1462-2920.14356.
23. Datta R, Ogeltree J. 1983. Methanol bioconversion by *Butyribacterium methylotrophicum*—batch fermentation yield and kinetics. Biotechnol Bioeng 25:991–998. https://doi.org/10.1002/bit.260250409.
24. Zeikus JG, Lynd LH, Thompson TE, Krzycki JA, Weimer PJ, Hegge PW. 1980. Isolation and characterization of a new, methylotrophic, acidogenic anaerobe, the Marburg strain. Curr Microbiol 3:381–386. https://doi.org/10.1007/BF02601907.
25. Worden RM, Grethlein AJ, Zeikus JG, Datta R. 1989. Butyrate production from carbon monoxide by *Butyribacterium methylotrophicum*. Appl Biochem Biotechnol 20-21:687–698. https://doi.org/10.1007/BF02936517.
26. Grethlein AJ, Worden RM, Jain MK, Datta R. 1991. Evidence for production of n-butanol from carbon monoxide by *Butyribacterium methylotrophicum*. J Ferment Bioeng 72:58–60. https://doi.org/10.1016/0922-338X(91)90147-9.
27. Shen GJ, Annous BA, Lovitt RW, Jain MK, Zeikus JG. 1996. Biochemical route and control of butyrate synthesis in *Butyribacterium methylotrophicum*. Appl Microbiol Biotechnol 45:355–362. https://doi.org/10.1007/s002530050696.

28. Lynd L, Kerby R, Zeikus JG. 1982. Carbon monoxide metabolism of the methylotrophic acidogen *Butyribacterium methylotrophicum*. J Bacteriol 149:255–263. https://doi.org/10.1128/jb.149.1.255-263.1982.
29. Bengelsdorf FR, Poehlein A, Schiel-Bengelsdorf B, Daniel R, Dürre P. 2016. Genome sequence of the acetogenic bacterium *Butyribacterium methylotrophicum* DSM 3468 T. Genome Announc 4:e01338-16. https://doi.org/10.1128/genomeA.01338-16.
30. Wang X, Qin J, Ma C, Wang J, Wang X, Xu S, Feng J, Chen K, Ouyang P. 2021. Methanol assimilation with CO_2 reduction in *Butyribacterium methylotrophicum* and development of genetic toolkits for its engineering. ACS Sustainable Chem Eng 9:12079–12090. https://doi.org/10.1021/acssuschemeng.1c02365.
31. Kim H, Jeon BS, Sang BI. 2019. An efficient new process for the selective production of odd-chain carboxylic acids by simple carbon elongation using *Megasphaera hexanoica*. Sci Rep 9:1–10. https://doi.org/10.1038/s41598-019-48591-6.
32. Huq NA, Huo X, Hafenstine GR, Tifft SM, Stunkel J, Christensen ED, Fioroni GM, Fouts L, McCormick RL, Cherry PA, McEnally CS, Pfefferle LD, Wiatrowski MR, Benavides PT, Biddy MJ, Connatser RM, Kass MD, Alleman TL, St John PC, Kim S, Vardon DR. 2019. Performance-advantaged ether diesel bioblendstock production by a priori design. Proc Natl Acad Sci U S A 116:26421–26430. https://doi.org/10.1073/pnas.1911107116.
33. Mahamkali V, Valgepea K, de Souza Pinto Lemgruber R, Plan M, Tappel R, Köpke M, Simpson SD, Nielsen LK, Marcellin E. 2020. Redox controls metabolic robustness in the gas-fermenting acetogen *Clostridium autoethanogenum*. Proc Natl Acad Sci U S A 117:13168–13175. https://doi.org/10.1073/pnas.1919531117.
34. Richter H, Molitor B, Wei H, Chen W, Aristilde L, Angenent LT. 2016. Ethanol production in syngas-fermenting: *Clostridium ljungdahlii* is controlled by thermodynamics rather than by enzyme expression. Energy Environ Sci 9:2392–2399. https://doi.org/10.1039/C6EE01108J.
35. Shen GJ, Shieh JS, Grethlein AJ, Jain MK, Zeikus JG. 1999. Biochemical basis for carbon monoxide tolerance and butanol production by *Butyribacterium methylotrophicum*. Appl Microbiol Biotechnol 51:827–832. https://doi.org/10.1007/s002530051469.
36. Leang C, Ueki T, Nevin KP, Lovley DR. 2013. A genetic system for *Clostridium ljungdahlii*: a chassis for autotrophic production of biocommodities and a model homoacetogen. Appl Environ Microbiol 79:1102–1109. https://doi.org/10.1128/AEM.02891-12.
37. Heap JT, Pennington OJ, Cartman ST, Minton NP. 2009. A modular system for *Clostridium* shuttle plasmids. J Microbiol Methods 78:79–85. https://doi.org/10.1016/j.mimet.2009.05.004.
38. Jeong J, Kim JY, Park B, Choi IG, Chang IS. 2020. Genetic engineering system for syngas-utilizing acetogen, *Eubacterium limosum* KIST612. Bioresour Technol Rep 11:100452. https://doi.org/10.1016/j.biteb.2020.100452.
39. Nguyen NPT, Raynaud C, Meynial-Salles I, Soucaille P. 2018. Reviving the Weizmann process for commercial n-butanol production. Nat Commun 9:3682. https://doi.org/10.1038/s41467-018-05661-z.
40. Seedorf H, Fricke WF, Veith B, Brüggemann H, Liesegang H, Strittmatter A, Miethke M, Buckel W, Hinderberger J, Li F, Hagemeier C, Thauer RK, Gottschalk G. 2008. The genome of *Clostridium kluyveri*, a strict anaerobe with unique metabolic features. Proc Natl Acad Sci U S A 105:2128–2133. https://doi.org/10.1073/pnas.0711093105.
41. Phillips JR, Atiyeh HK, Tanner RS, Torres JR, Saxena J, Wilkins MR, Huhnke RL. 2015. Butanol and hexanol production in *Clostridium carboxidivorans* syngas fermentation: medium development and culture techniques. Bioresour Technol 190:114–121. https://doi.org/10.1016/j.biortech.2015.04.043.
42. Huq NA, Hafenstine GR, Huo X, Nguyen H, Tifft SM, Conklin DR, Stück D, Stunkel J, Yang Z, Heyne JS, Wiatrowski MR, Zhang Y, Tao L, Zhu J, McEnally CS, Christensen ED, Hays C, van Allsburg KM, Unocic KA, Meyer HM, Abdullah Z, Vardon DR. 2021. Toward net-zero sustainable aviation fuel with wet waste–derived volatile fatty acids. Proc Natl Acad Sci U S A 118:e2023008118. https://doi.org/10.1073/pnas.2023008118.
43. Chen WS, Ye Y, Steinbusch KJJ, Strik D, Buisman CJN. 2016. Methanol as an alternative electron donor in chain elongation for butyrate and caproate formation. Biomass Bioenergy 93:201–208. https://doi.org/10.1016/j.biombioe.2016.07.008.
44. Lynd LH, Zeikus JG. 1983. Metabolism of H_2-CO_2, methanol, and glucose by *Butyribacterium methylotrophicum*. J Bacteriol 153:1415–1423. https://doi.org/10.1128/jb.153.3.1415-1423.1983.
45. Heiskanen H, Virkajärvi I, Viikari L. 2007. The effect of syngas composition on the growth and product formation of *Butyribacterium methylotrophicum*. Enzyme Microb Technol 41:362–367. https://doi.org/10.1016/j.enzmictec.2007.03.004.
46. Kerby R, Zeikus JG. 1987. Anaerobic catabolism of formate to acetate and CO_2 by *Butyribacterium methylotrophicum*. J Bacteriol 169:2063–2068. https://doi.org/10.1128/jb.169.5.2063-2068.1987.
47. Nicholls P. 1975. Formate as an inhibitor of cytochrome c oxidase. Biochem Biophys Res Commun 67:610–616. https://doi.org/10.1016/0006-291x(75)90856-6.
48. Pfeifenschneider J, Brautaset T, Wendisch VF. 2017. Methanol as carbon substrate in the bio-economy: metabolic engineering of aerobic methylotrophic bacteria for production of value-added chemicals. Biofuels Bioprod Bioref 11:719–731. https://doi.org/10.1002/bbb.1773.
49. Müller V, Chowdhury NP, Basen M. 2018. Electron bifurcation: a long-hidden energy-coupling mechanism. Annu Rev Microbiol 72:331–353. https://doi.org/10.1146/annurev-micro-090816-093440.
50. Bertsch J, Müller V. 2015. Bioenergetic constraints for conversion of syngas to biofuels in acetogenic bacteria. Biotechnol Biofuels 8:210. https://doi.org/10.1186/s13068-015-0393-x.
51. Chen PYT, Aman H, Can M, Ragsdale SW, Drennan CL. 2018. Binding site for coenzyme A revealed in the structure of pyruvate:ferredoxin oxidoreductase from *Moorella thermoacetica*. Proc Natl Acad Sci U S A 115:3846–3851. https://doi.org/10.1073/pnas.1722329115.
52. Weghoff MC, Bertsch J, Müller V. 2015. A novel mode of lactate metabolism in strictly anaerobic bacteria. Environ Microbiol 17:670–677. https://doi.org/10.1111/1462-2920.12493.
53. Jin S, Bae J, Song Y, Pearcy N, Shin J, Kang S, Minton NP, Soucaille P, Cho B-K. 2020. Synthetic biology on acetogenic bacteria for highly efficient conversion of C1 gases to biochemicals. Int J Mol Sci 21:7639. https://doi.org/10.3390/ijms21207639.
54. Flüchter S, Follonier S, Schiel-Bengelsdorf B, Bengelsdorf FR, Zinn M, Dürre P. 2019. Anaerobic production of poly(3-hydroxybutyrate) and its precursor 3-hydroxybutyrate from synthesis gas by autotrophic Clostridia. Biomacromolecules 20:3271–3282. https://doi.org/10.1021/acs.biomac.9b00342.
55. Woolston BM, Emerson DF, Currie DH, Stephanopoulos G. 2018. Rediverting carbon flux in *Clostridium ljungdahlii* using CRISPR interference (CRISPRi). Metab Eng 48:243–253. https://doi.org/10.1016/j.ymben.2018.06.006.
56. Marcano-Velazquez JG, Lo J, Nag A, Maness PC, Chou KJ. 2019. Developing riboswitch-mediated gene regulatory controls in thermophilic bacteria. ACS Synth Biol 8:633–640. https://doi.org/10.1021/acssynbio.8b00487.